DEUTSCHES ELEKTRONEN-SYNCHROTRON DESY

DESY SR-82-13
September 1982

PARTIAL PHOTOIONIZATION CROSS-SECTIONS OF RARE EARTHS METALS IN THE REGION OF THE 4d RESONANCE

by

F. Gerken, J. Barth and C. Kunz

II. Inst. für Exp. Physik, Universität Hamburg

NOTKESTRASSE 85 · 2 HAMBURG 52

To be sure that your preprints are promptly included in the
HIGH ENERGY PHYSICS INDEX ,
send them to the following address (if possible by air mail) :

DESY
Bibliothek
Notkestrasse 85
2 Hamburg 52
Germany

DESY SR-82-13
September 1982

PARTIAL PHOTOIONIZATION CROSS-SECTIONS OF RARE EARTHS METALS IN THE REGION OF THE 4d RESONANCE

F. Gerken, J. Barth and C. Kunz
II. Inst. f. Exp. Phys., Universität Hamburg, Luruper Chaussee 149
2000 Hamburg 50, FRG

ABSTRACT

The partial photoionization cross-sections of the 4d-, 5p-, 4f-shells and the valence band of Ce, Pr, Nd, Eu and Gd are measured in the region of the 4d→4f excitation. The sum is compared with the corresponding absorption spectrum in order to estimate the importance of different decay channels of the excited $4d^9 4f^{N+1}$ configurations. For the heavy rare earth metals, which show a large 4f multiplet splitting, we demonstrate that the coupling of the 4f ionization to the 4d→4f excitations strongly depends on the particular $(4f^{N-1})\ ^{2S+1}L_J$ - multiplet lines. This effect is also discussed for the 5p multiplet lines in Eu which arise from the coupling of the 5p hole with the 4f electrons.

INTRODUCTION

The partially filled and localized 4f shell in the rare earths gives rise to many interesting problems in different physical fields. The absorption spectra in the region of the 4d excitation show a number of sharp lines followed by a large maximum over an energy range of 10 to 20 eV [1]. These spectra, similar for rare earth atoms and solids [2], could be explained by excitations into bound 4f states [3] with a large multiplet splitting of the excited $4d^9 4f^{N+1}$ configuration [2,4]. Strong intershell interactions in the region of the 4d→4f excitation have been well established in photoemission experiments by use of synchrotron radiation ("resonant photoemission"). The partial photoionization cross-sections (PPCS's) show intensity variations which can be described by the Fano-theory [5,6,7]. For barium, which has no 4f electron in the ground state, the PPCS's of the 4d, 5p and 5s shell have been measured by Hecht and Lindau[8] at the 4d threshold and the results are compared with several calculations. For the 4d- and 5p-cross-sections the best agreement was found for RPAE calculations by Amusia[9] and by Wendin[10]. The theoretical understanding of the subshell cross-sections at the 4d threshold is quite satisfactory for the elements without 4f electrons (Ba and La) for which a consistent interpretation of alternative calculation procedures could be given by Wendin and Starace [11].

For the rare earths with a partially filled 4f shell the theoretical description is much more complicated. For Ce, which has one electron in the 4f shell in the ground state, Zangwill and Soven[12] presented a calculation of the different PPCS in a time dependent local density approximation. We have measured the 4d-, 5p-, 4f-shells and valence band cross-sections for Ce, Pr, Nd, Eu and Gd which show a relatively simple 4f-multiplet structure in photo-

Contribution to the International Conference on X-Ray and Atomic Inner-Shell Physics, Eugene, Oregon, USA (1982), to be published in the American Institute of Physics Conference Proceedings

emission spectra. Since the sum of all PPCS's gives the total absorption coefficient, the individual importance of the different contributions can be estimated. For the rare earths with a large 4f multiplet splitting our high resolution photoemission spectra demonstrate that the coupling of the 4f ionization to the 4d→4f excitation strongly depends on the particular $(4f^{N-1})\ ^{2S+1}L_J$-multiplet line. This is shown as an example for Er and Tm. This effect is also observed for the 5p multiplet lines which arise from the coupling of the 5p hole with the partially filled 4f shell and will be discussed for Eu.

EXPERIMENTAL PROCEDURE

Our measurements were performed at the Hamburger Synchrotronstrahlungslabor HASYLAB with the monochromator FLIPPER. Details of the experimental setup are given elsewhere [13]. The samples were evaporated in situ from tungsten baskets under UHV conditions onto stainless steel substrates. The spectra presented here are normalized to the incoming photon flux which was monitored with a Au-photodiode [14]. The cylindrical mirror analyser was used in the retarding mode (ΔE=const.) to allow the measurement of high resolution CIS-spectra from narrowlyspaced structures. The spectra are corrected for the analyser transmission by a new method described in ref. 14. The influence of the mean free path to the PPCS has been omitted since the variation of the mean free path is small in the energy range of interest [15]. The different PPCS's are measured continuously by use of Constant-Initial-State (CIS) spectroscopy.

Although we used ultrapure materials (rare earth products 99.99 %) which we evaporated in ultrahigh vacuum ($\sim 1.10^{-10}$ Torr) a small contamination signal at about 6 eV binding energy was detectable on all samples. Auger measurements of the samples show that this contaminations are mainly oxygen and chlorine which are probably residuals from the technical production process [16]. We can estimate the coverage to be less than 0.1 monolayer if we take into account that our measurements are extremely surface sensitive. Therefore we do not expect an influence of the contaminations to the PPCS's of interest.

RESULTS AND DISCUSSION

The data analysis for the PPCS-measurements is the same for all materials and shall be described in detail only for Ce. Fig. 1 shows a series of Electron Distribution Curves (EDC) for photon energies in the region of the 4d excitation. The Ce spectra show a double structure with maxima at 0.5 eV and 2 eV binding energy. It is still a matter of discussion whether only the 2 eV peak or both structures have 4f character [6,17,18,19,20]. Both peaks show drastic intensity variations when the photon energy is tuned to the region of the 4d→4f excitation. This phenomenon is usually described as a direct

recombination of the excited state resulting from a process such as
$4d^{10}5s^25p^64f^NV \rightarrow 4d^95s^25p^64f^{N+1}V \rightarrow 4d^{10}5s^25p^64f^{N-1}V\epsilon\ell$

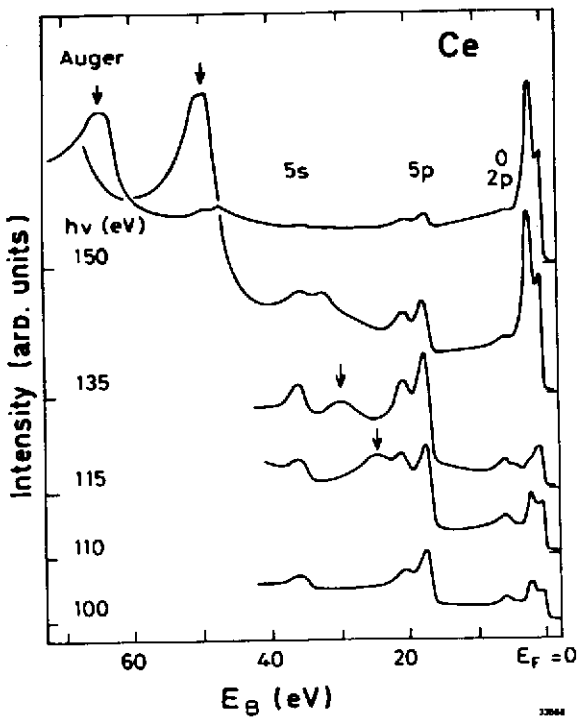

Fig. 1: EDC's of Ce metal in the region of the 4d → 4f excitation. The spectra are normalized to the photon flux. The arrows indicate the main Auger peak.

V stands for the valence band 5d- and 6s-electrons. The process given above interferes with the direct photoemission from the 4f shell. The resulting intensity profile can be described by the Fano interference formalism[6,17].

Apart from this process the energy from the direct recombination may be transferred to electrons from the other outer shells resulting in processes such as

$$4d^95s^25p^64f^{N+1}V \rightarrow \begin{cases} 4d^{10}5s\ 5p^64f^NV\epsilon\ell \\ 4d^{10}5s^25p^54f^NV\epsilon\ell \\ 4d^{10}5s^25p^64f^NV^{(-1)}\epsilon\ell \\ 4d^95s^25p^64f^NV\epsilon\ell \end{cases}$$

The last decay is equivalent to the direct photoemission of the 4d electron. The 4d hole decays via an Auger process leading to an Auger structure in the spectra at fixed kinetic energy. In Fig. 1 the main Auger peak is indicated by an arrow. The intensity of the Auger peak should be directly proportional to the number of 4d holes. From Fig. 1 it is obvious that this autoionisation process is an important competition compared to the direct recombination processes.

In order to determine the relative intensities of all PPCS's we have measured CIS-spectra from the structures with E_B = 0,5 eV and E_B = 2 eV and the $5p$ structure with the lowest binding energy and normalized these spectra to the corresponding peak areas as shown in Fig. 2. For each structure the background of inelastically scattered electrons which is created by the other structures at lower binding energies is considered by subtraction of a CIS-sprectrum of the preceding background at lower initial energy.

Since the direct 4d emission near threshold is superimposed on the very steep background of scattered electrons at low kinetic energies, this channel could not be obtained with high accuracy by CIS-spectroscopy. In order to solve this problem we have measured a series of Constant-Final-State (CFS) spectra, where the electron

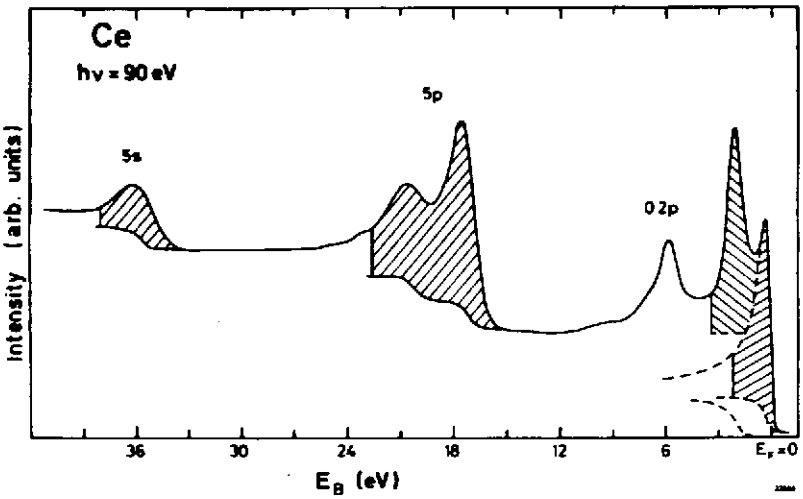

Fig. 2: EDC of Ce metal measured with a photon energy of 9o eV indicating the peak areas which are used for the correction of the CIS-spectra

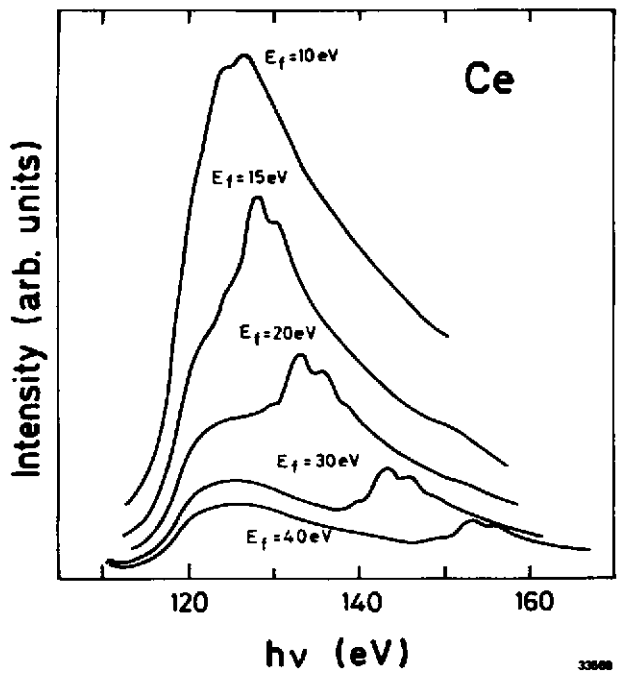

Fig. 3: Series of CFS-spectra of Ce metal with different final energies E_f. The 4d emission is superimposed on the absorption structure and shifts on the photon energy scale when changing the final energy

analyser is fixed to a constant final energy E_f while the photon energy is varied. The result for five different final energies is shown in Fig. 3. In such spectra the shape of the background is proportional to the absorption structure independently of the analyser's final energy. The contribution from the direct 4d emission appears at different photon energies superimposed on this background and can be much easier extracted. At threshold the Auger intensity serves to estimate the 4d-PPCS. In Fig. 4 the different PPCS's are compared with the absorption structure which was measured using the partial yield technique, i.e., by measuring the yield of low-energy electrons as a function of photon energy. The 4f-, 5p, E_B = o.5 eV- and E_B = 2 eV PPCS's which are continuously measured by CIS- spectroscopy are subtracted from the total yield ("a-b" in Fig. 4). The remaining part agrees well with the data points obtained for the 4d-PPCS. The 5s-PPCS could not be determined because of overlapping Auger structures for excitation energies within the giant resonance. This fact may explain the remaining small

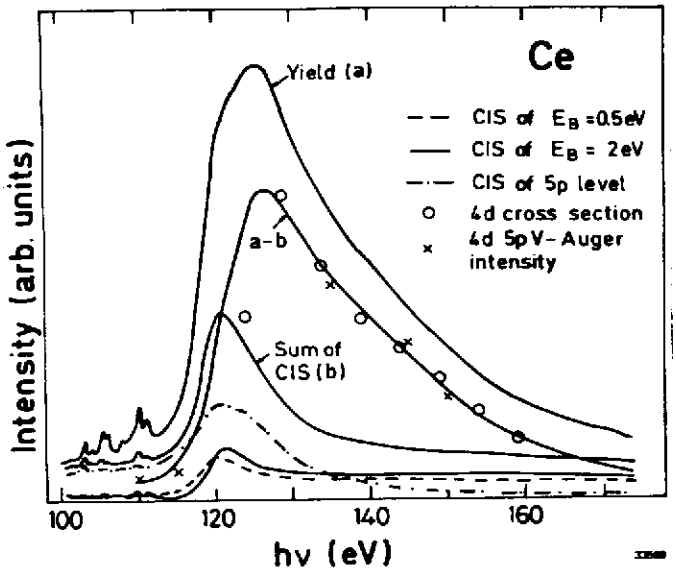

Fig. 4: Different partial photoionization cross-sections (PPCS's) for Ce metal. The sum of the E_B = 0.5 eV-, E_B = 2 eV- and 5p- PPCS's (b) is substracted from the yield spectrum (a) and the remaining part (a-b) is in good agreement with the obtained points for the 4d-PPCS.

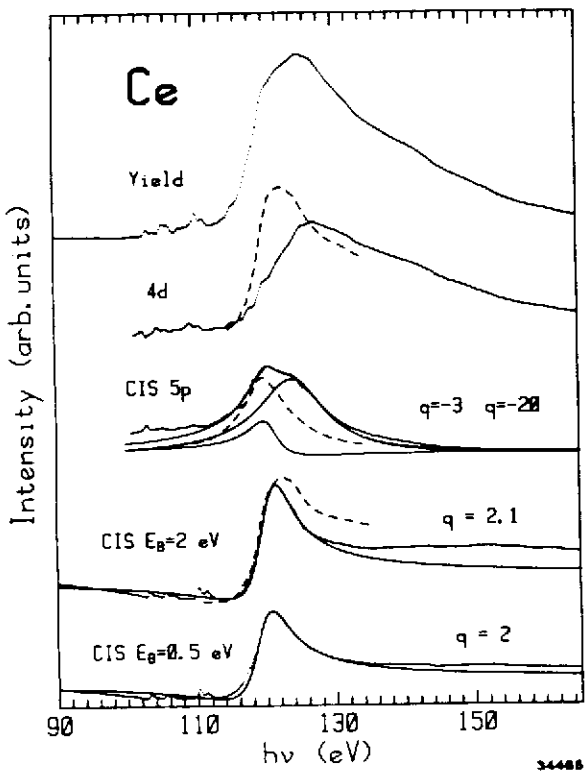

Fig. 5: Line shapes of the different PPCS's for Ce metal on an arbitrary scale ....:experimental data, ——: fitted Fano-profiles with given q-values, ----:theory of Zangwill and Soven[12].

deviations between the sum of all measured PPCS's and the yield since the 5s PPCS must be expected to be of comparable magnitude to the valence band-PPCS. The 4d-PPCS is by far the most dominant part of all PPCS's for Ce and is obviously responsible for the high energy part of the absorption structure while the preceding shoulder is reproduced by the enhancement of the cross-sections of the outer levels. Apart from the relative intensities it is interesting to note the dissimilar line shapes of the different PPCS's from Fig. 5. While the two structures with E_B = 0.5 eV and E_B = 2 eV can be fitted quite well by a single Fano-profile with a positive q-value, the 5p-PPCS consists of at least two curves with negative q-values and peak-positions corresponding to the double-structure of the absorption profile. Our results can be compared with the calculation of Zangwill and Soven[12] in the TDLDA. The relative inten-

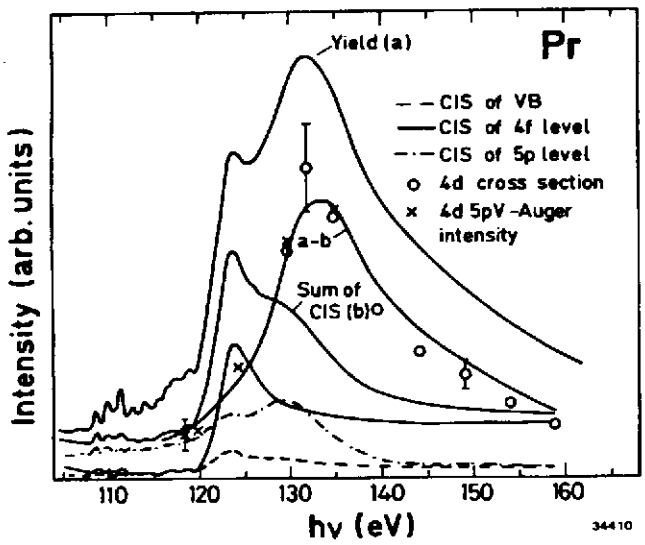

Fig. 6: Different PPCS's for Pr metal analysed in the same way as for Ce metal (see Fig. 4)

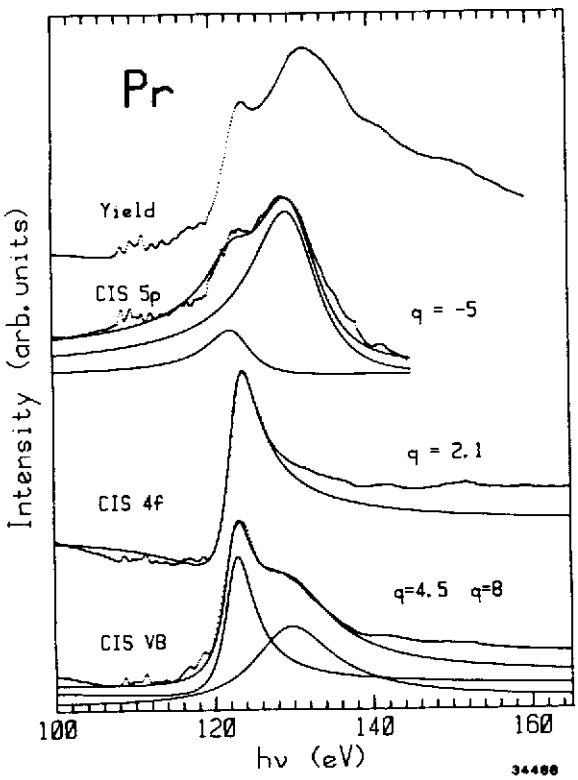

Fig. 7: Like shapes of the different PPCS's for Pr metal on an arbitrary scale ....: experimental data, ——: fitted Fano profile with given q-values

sities of their calculation are in agreement with our results with respect to the experimental error which is mainly caused by the difficult determination of the exact peak areas for the normalization of the CIS spectra. This is due to the rich multiplet splitting of the 5p- and 4d core levels in the photoemission spectra. On the other hand the calculated line shapes and peak positions are in distinct contradiction to our results (see Fig. 5). The 4d- and 4f PPCS's differ in line shapes as well as in the position of the maxima ($\sim$ 4 eV) while Zangwill and Soven emphasize the similarity of the energy dependence of both PPCS. Furthermore, the theory is unable to explain the double-structure of the 5p-PPCS which is obviously coupled to different multiplet lines of the absorption curve. We can compare our results for Ce with an analysis of our Pr data. Pr is the following element of the rare earths with two 4f electrons in the ground state. The

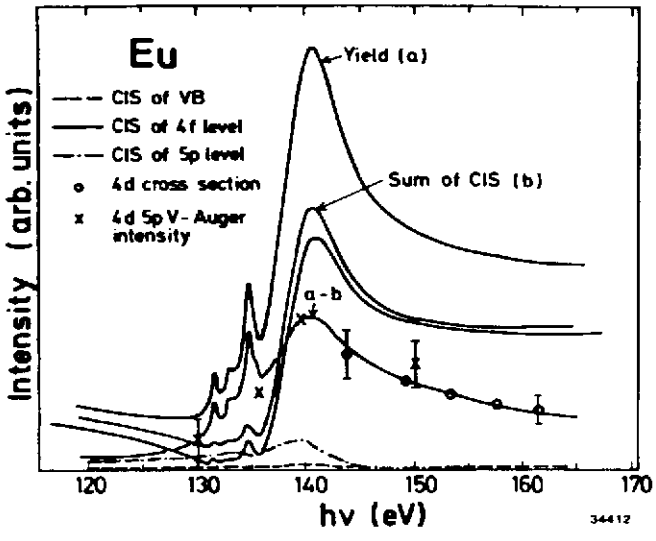

Fig. 8: Different PPCS's for Eu metal analysed in the same way as for Ce metal (see Fig. 4)

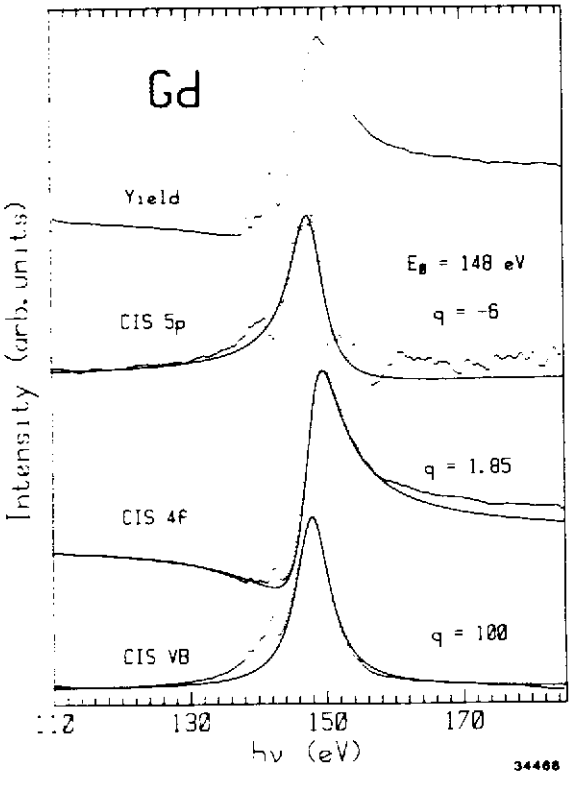

Fig. 9: Line shapes of the different PPCS's for Gd metal on an arbitrary scale
....: experimental data,
——: fitted Fano profile with given q-values. The given resonance energy E_0 is the same for all PPCS. The relatively high statistics in the 5p CIS sprectrum above 15o eV is due to the very low count rate of the subtracted CIS sprectra (5p and preceding background).

4f emission appears at about 3.5 eV binding energy in the photoemission spectra. The different PPCS's in the region of the 4d → 4f excitation are shown in Fig. 6.

Similar to Ce the absorption-curve of Pr consists of a double structure in the giant maximum but the separation of the peaks is significantly larger in Pr. While the relative intensities of the different PPCS's changed from Ce to Pr, the line shapes are comparable (see Fig. 6 and Fig. 7). Again the 4d-PPCS coincides with

	valence band				4f				5p			
	relative intensity	E_o (eV)	Γ (eV)	q	relative intensity	E_o (eV)	Γ (eV)	q	relative intensity	E_o (eV)	Γ (eV)	q
Ce	80	119.25	2.9	2	100	120.05	2.8	2.1	200	120.6	2.5	- 3
										124.3	6	-20
Pr	20	122.6	2.2	4.5	100	122.6	2.4	2.0	60	123	3.3	- 5
		129	6	8						130.5	5.0	- 5
Eu	2.5	138.2	3.7	5	100	138.9	3.0	1.45	13	140.5	2.75	- 3
Gd	3	148	3	100	100	148	3	1.85	10	148	3	- 6

Table 1: Fit parameter for the Fano-profiles for Ce, Pr, Eu and Gd. The relative intensities of the different PPCS refer to the intensity in the maximum of the giant resonance relative to the intensity of the 4f level (E_B = 2 eV in Ce) which is arbitrarely chosen to be 100 in each case.

the high energy maximum of the yield. The 4f-PPCS only contributes to the onset of the giant resonance and can be well fitted by a single Fano-profile. The valence band- and 5p-PPCS's are coupled to the whole absorption structure and can be fitted by a sum of two Fano-profiles each with negative q-values for the 5p- and positive q-values for the valence band PPCS. The significantly lower q-value for the first Fano-profile of the valence band-PPCS in Pr compared to the second one may be caused by an overlap of the relatively broad 4f multiplet lines (HWHM $\triangleq$ 0.4 eV) with the preceding valence band resulting in a mixture of 4f- and VB-PPCS in the measured CIS-spectrum.

The line shapes for the different PPCS's discussed above appear to be independent of the material. This is confirmed by the analysis for Nd, Eu and Gd: negative q-values for the 5p-PPCS's, low positive q-values for the 4f-PPCS's and high positive (nearly Lorentzian-like) q-values for the valence-band PPCS's (see Table 1). Especially the elements in the middle of the rare earths series, Eu and Gd which both have a half filled 4f shell in the ground state, are a good example for the different PPCS-line shapes. The width of the absorption structure decreases from 2o eV to about 1o eV for the heavy rare earths (from Eu to Tm) resulting in PPCS's with a single peak in the giant absorption maximum. Here, the peak positions are nearly the same for all different PPCS's. Their relative intensities change continuously from Ce to Gd. The data analysis for Eu in Fig. 8 shows the increasing importance of the 4f-PPCS compared to the lighter rare earths. In Fig. 9 the different line shapes of the PPCS's in Gd are presented on an arbitrary intensity scale. In Gd the valence band and the 4f level are well separated by about 8 eV in the photoemission spectrum. This provides an easy determination of the PPCS's without mixing of different levels. In this case the valence band PPCS can be fitted with an almost Lorentzian curve.

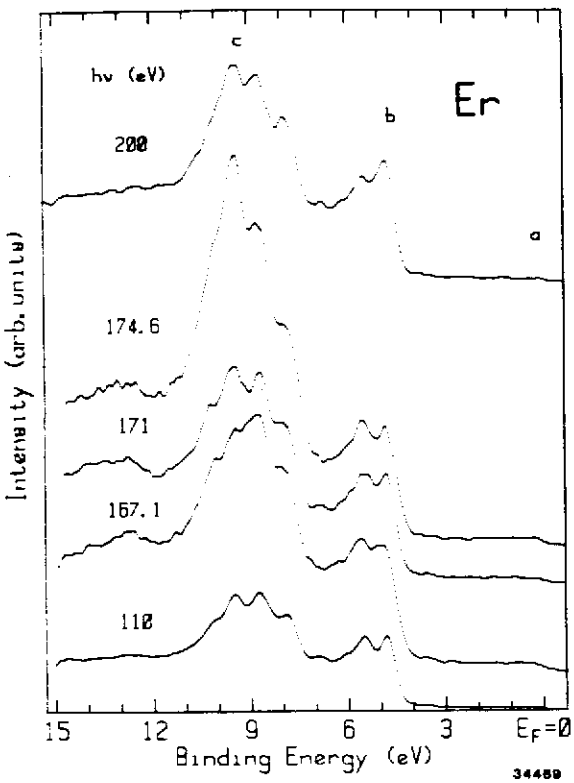

Fig. 10: Series of EDC's of Er metal showing the valence band region with the rich multiplet structure of the $4f^{11} \rightarrow 4f^{10}$ transition between 4 eV and 15 eV binding energy. A drastic change in the relative intensities of the different multiplet structures appears when the photon energy is scanned to the region of the 4d → 4f excitation

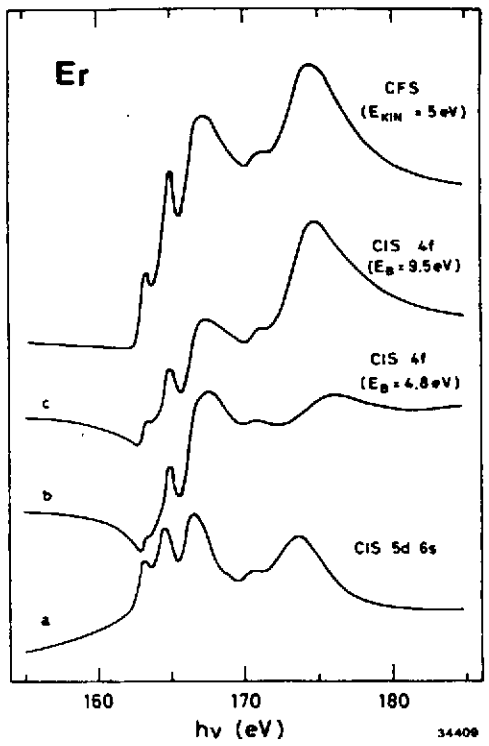

Fig. 11: CIS spectra of two different 4f multiplet lines (b and c from Fig. 10) and from the 5d6s-valence band (a) compared with a CFS which is proportional to the absorption structure

Comparing the results of Ce, Pr, Nd, Eu and Gd it is striking that only for Ce the line shapes of the two structures with E_B = 0.5 eV and E_B = 2 eV are very similar and both show a 4f-like resonance, e.g. there is no structure in the Ce spectra which shows the same behaviour as the 5d6s-valence electrons from the other materials. Since we have no reasons to expect the 5d6s-electrons in Ce to be totally different from the other elements we come to the conclusion that there is also 4f character in both the E_B = 0.5 eV and E_B = 2 eV peaks. Indeed, it is also possible to fit the Ce CIS-spectrum of the peak with E_B =0.5 eV with a sum of a Lorentzian and a Fano profile which corroborates with the expectation that the E_B = 0.5 eV peak consists of a 5d6s- and a 4f-part.

The data analysis presented here comprises only the most important decay channels in the 4d → 4f excitation range. We neglect

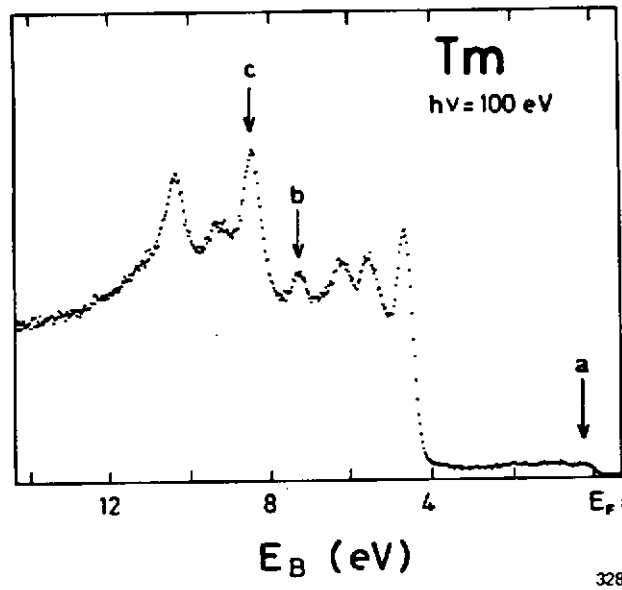

Fig. 12: EDC of Tm metal at 100 eV photon energy showing the multiplet structure of the $4f^{12} \rightarrow 4f^{11}$ transition (experimental resolution: 0.2 eV). The letters refer to the CIS spectra in Fig. 13

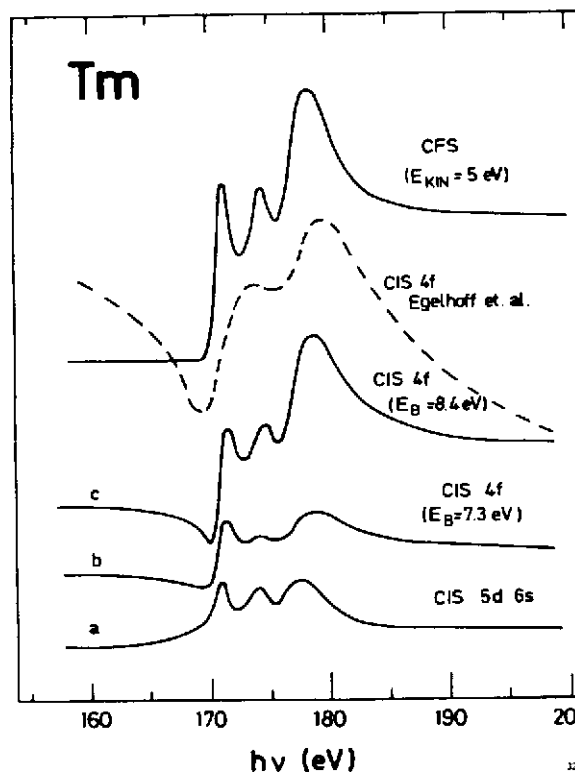

Fig. 13: CIS spectra of two different 4f multiplet lines (b and c) and from the 5d6s-valence band (a) from Tm metal compared with a CFS and a 4f CIS spectrum from Ref. 22 (dashed curve).

smaller effects such as the appearance of additional multiplet lines [21] and different PPCS's for the different $(4f^{N-1})^{2S+1}L_J$ multiplets which influence the sum of all PPCS's mainly in the region of the absorption fine structure preceding the giant maximum. The latter effect can easily be studied on heavy rare earth metals if monochromator and spectrometer are operated with high resolution. Fig. 10 shows a series of EDC's of Erbium (ground state $4f^{11}$) around the 4d → 4f resonance. A dramatic change in the relative intensities of the 4f multiplets lines occurs when the photon energy is tuned to the region of the 4d → 4f excitation. Fig. 11 presents CIS-spectra of the valence band and two different 4f multiplet lines as indicated in Fig. 10 compared with an absorption curve (CFS in Fig. 11). Equivalent measurements for Tm are presented in Fig. 13. The different 4f-CIS spectra refer to two neighbouring

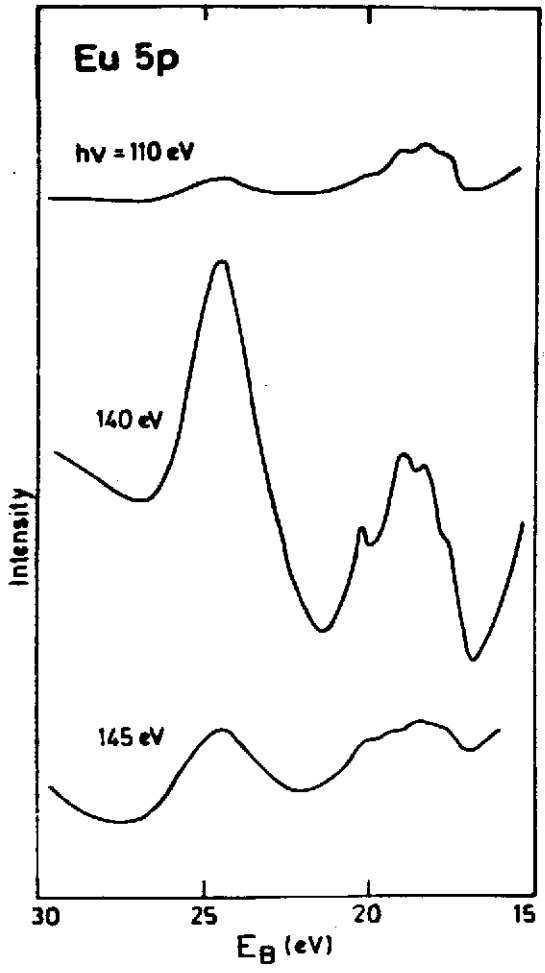

Fig. 14: EDS's of the 5p multiplet lines in Eu for photon energies below and within the 4d resonance. The spectra are measured with zero-suppresion. The amplitudes are normalized to the incoming photon flux. A dramatic change in the relative multiplet intensities appears in the region of the 4d resonance

4f multiplet lines in Fig. 12. We note that also for the heavy rare earths the CIS spectra of the 5d6s valence electrons clearly show almost Lorentzian profiles.

Our results for Tm are compared with a recent measurement from Egelhoff et al.[22] obtained with obviously reduced resolution demonstrating the importance of measuring these spectra with high resolving power.

The theoretical description of these effects is complicated but Davis[23] succeeded in calculating the PPCS's of the different $(4f^{12})^{2S+1}L_J$ multiplet-lines in Yb_2O_3 in the 4d → 4f excitation range. The sum of this different PPCS's is in good agreement with an experimental result from Johansson et al.[24]

Finally Fig. 14 shows a series of EDC's of the Eu-5p-core level for excitation energies below and within the 4d-resonance. The photoemission of a 5p-electron in the RE results in a coupling of the 5p-hole to the partially filled 4f-shell which leads to a complicated multiplet structure. The simplest case is given for the half filled 4f-shell in Eu with 6 possible final states: $4f^7(^8S_{7/2})5p^5\ ^{7,9}P_J$. It is obvious from Fig. 14 that the coupling of the individual 5p multiplet lines in the EDC's to the individual 4d → 4f resonant states differs. In this respect the result is similar to that obtained for the 4f-multiplets on the heavy rare earths. For Gd which has the same number of 4f electrons the result is completely equivalent to Eu. For the other rare earths we find the same behaviour.

CONCLUSION

We have shown that the main absorption structures of the rare earths in the region of the 4d → 4f excitation can be composed by the sum of the different outer shell PPCS, e.g. there are no important decay channels which lead to satellite structures of considerable intensity as observed in the elements of the 3d-series.[15,25,26] The relative intensities of the different $^{2S+1}L_J$ final state multiplet lines are strongly influenced by the intershell interaction. This has been demonstrated for the $4f^{10}$ multiplets in Er and the $4f^{11}$ multiplets in Tm as well as for the 5p multiplet lines in Eu which arise from the coupling of a 5p-hole with the partially filled 4f shell. These effects as well as the appearance of additional multiplet lines[19] influence the sum of the PPCS mainly in the fine structure of the absorption. For Tm it was possible to correct previous errors in the 4f resonance spectra of other authors[22] by our high resolution measurements. A further improvement of our experimental set-up which is now in preparation will in future allow an even more detailled analysis including all effects described above in the measurements of the PPCS and therefore will provide even deeper insight into the intershell interactions in the rare earth resonances. The theoretical understanding of the resonant photoemission in the rare earth is in the beginning stage and we hope that our results may stimulate a futher progress in this field.

REFERENCES

1. T.M. Zimkina, V.A. Fomichev, S.A. Gribovskii and I.I. Zhukova, Fiz. Tverd. Tela 9, 1447 (1967) Sov. Phys. Solid State 9, 1128 (1967)

2. H.W. Wolff, R. Bruhn, K. Radler and B. Sonntag, Phys. Lett. 59A, 67 (1976)

3. J.L. Dehmer, A.F. Starace, U. Fano, J. Sugar and J.W. Cooper, Phys. Rev. Lett. 26, 1521 (1971)

4. J. Sugar, Phys. Rev. B5, 1785 (1972)

5. W. Lenth, F. Lutz, J. Barth, G. Kalkoffen and C. Kunz, Phys. Rev. Lett. 41, 1185 (1978)

6. L.I. Johansson, J.W. Allen, T. Gustafsson, I. Lindau and S.B. Hagström, Solid State Commun. 28, 53 (1978)

7. F. Gerken, J. Barth, K.L.I. Kobayashi and C. Kunz, Solid State Commun. 35, 179 (198o)

8. M. Hecht and I. Lindau, Phys. Rev. Lett. 47, 821 (1981)

9. M.Y. Amusia, V.K. Ivanov, L.V. Chernysheva, Phys. Lett. 59A, 191 (1979)

1o. G. Wendin in VUV Radiation Physics, edited by E.E. Koch et al. (Vieweg-Pergamon, Berlin, 1974) p. 225

11. G. Wendin and A.F. Starace, J. Phys. B11, 4119 (1978)

12. A. Zangwill and P. Soven, Phys. Rev. Lett. 45, 2o4 (198o)

13. J. Barth, F. Gerken, J. Schmidt-May and C. Kunz, Contribution to the Synchrotron Radiation Instrumentation (SRI) Conference, Hamburg, 1982, to be published in Nucl. Instr. and Methods

14. J. Barth, F. Gerken and C. Kunz, Contribution to the SRI Conference, Hamburg, 1982, to be published in Nucl. Instr. and Methods

15. J. Barth, Thesis, University of Hamburg (1982)

16. A. Platau, Thesis, University of Linköping, Sweden (1982)

17. G. Kalkoffen, Thesis, University of Hamburg, Germany (1978)

18. D. Wieliczka, J.H. Weaver, D.W. Lynch and C.G. Olson, to be published

19. S.H. Lin and K.-M. Ho, to be published

2o. S. Hüfner and P. Steiner, Zeitschrift f. Phys. B46, 37 (1982)

21. F. Gerken, J. Barth and C. Kunz, Phys. Rev. Lett. 47, 993 (1981)

22. W.F. Egelhoff, E.E. Tibbetts, M.H. Hecht and I. Lindau, Phys. Rev. Lett. 46, 1o71 (1981)

23. L.C. Davis, to be published

24. L.I.Johansson, J.W. Allen, I. Lindau, M.H. Hecht and S.B.M. Hagström, Phys. Rev. B21, 14o8 (198o)

25. J. Barth, F. Gerken, K.L.I. Kobayashi, J.H. Weaver and B. Sonntag, J. Phys. C13, 1369 (198o)

26. J. Barth, F. Gerken and C. Kunz, to be published